https://doi.org/10.5194/essd-2019-246
Preprint. Discussion started: 27 January 2020

The fate of land evaporation – A global dataset

Andreas Link[1], Ruud van der Ent[2,3], Markus Berger[1], Stephanie Eisner[4], Matthias Finkbeiner[1]

[1]Chair of Sustainable Engineering, Technical University of Berlin, Berlin, 10623, Germany
[2]Department of Water Management, Faculty of Civil Engineering and Geosciences, Delft University of Technology, Delft, Netherlands
[3]Department of Physical Geography, Faculty of Geosciences, Utrecht University, Utrecht, Netherlands
[4]Norwegian Institute of Bioeconomy Research, Ås, 1431, Norway

Correspondence to: Andreas Link (andreas.link@tu-berlin.de)

Abstract. Various studies investigated the fate of evaporation and the origin of precipitation. The more recent studies among them were often carried out with the help of numerical moisture tracking. Many research questions could be answered within this context such as dependencies of atmospheric moisture transfers between different regions, impacts of land cover changes on the hydrological cycle, sustainability related questions as well as questions regarding the seasonal and inter-annual variability of precipitation. In order to facilitate future applications, global datasets on the fate of evaporation and the sources of precipitation are needed. Since most studies are on a regional level and focus more on the sources of precipitation, the goal of this study is to provide a readily available global dataset on the fate of evaporation for a fine-meshed grid of source and receptor cells. The dataset was created through a global run of the numerical moisture tracking model WAM-2layers and focused on the fate of land evaporation. The tracking was conducted on a 1.5° × 1.5° grid and was based on reanalysis data from the ERA-Interim database. Climatic input data were incorporated in 3- respectively 6-hourly time steps and represent the time period from 2001 to 2018. Atmospheric moisture was tracked forward in time and the geographical borders of the model were located at +/- 79.5° latitude. As a result of the model run, the annual and monthly average as well as the inter-annual average fate of evaporation was determined for 8684 land grid cells (all land cells except those located within Greenland and Antarctica) and provided via source-receptor matrices. The gained dataset was complemented via an aggregation to country and basin scales in order to highlight possible usages for areas of interest larger than grid cells. This resulted in data for 265 countries and 8223 basins. Finally, five types of source-receptor matrices for average moisture transfers were chosen to build the core of the dataset: land grid cell to grid cell, country to grid cell, basin to grid cell, country to country, basin to basin. The dataset is, to our knowledge, the first ready-to-download dataset providing the overall fate of evaporation for land cells of a global fine-meshed grid in monthly resolution. At the same time, information on the sources of precipitation can be extracted from it. It could be used for investigations into average annual, seasonal and inter-annual sink and source regions of atmospheric moisture from land masses for most of the regions in the world and shows various application possibilities for studying interactions between people and water such as land cover changes or human water consumption patterns. The dataset is accessible under https://doi.pangaea.de/10.1594/PANGAEA.908705 (Link et al., 2019a) and comes along with example scripts for reading and plotting.

https://doi.org/10.5194/essd-2019-246
Preprint. Discussion started: 27 January 2020

1) Introduction

Where does evaporated water go to and where is the origin of precipitation? This question has been addressed by more and more studies within the last decades as demonstrated in more detail below. In order to describe the fate of evaporation or the source of precipitation the concept of atmospheric watersheds was developed in which the terms "evaporationshed" (Van der Ent and Savenije, 2013) and "precipitationshed" (Keys et al., 2012) were introduced. According to van der Ent (2014) "an evaporationshed describes the downwind atmosphere and surface that receives precipitation from a specific location's evaporation" whereas "a precipitationshed is defined as the upwind atmosphere and surface that contributes evaporation to a specific location's precipitation".

Several methods are available to identify the origin and fate of moisture such as analytic box models as well as physical and numerical (Eulerian and Lagrangian) moisture tracking models (Gimeno et al., 2012). Particularly relevant for large scale studies are numerical moisture tracking models which were used in the majority of the more recent studies within this field (Dominguez et al., 2019; Van der Ent et al., 2013; Gimeno et al., 2012). Those models show various application opportunities of which some of the main applications are listed as well as partly exemplified below:

1. Gaining increased knowledge on how regions of interest are dependent of the moisture supply from other regions (Bagley et al., 2012; Dirmeyer et al., 2009; Dominguez et al., 2016; Guo et al., 2019; Keune and Miralles, 2019; Keys et al., 2012, 2018; Salih et al., 2016; Staal et al., 2018; Zhao et al., 2016, 2019)
2. Understanding land cover changes and its impacts on the supply of moisture to downwind beneficiaries (Bagley et al., 2012; Keys et al., 2012, 2018; Spracklen et al., 2012; Staal et al., 2018; Tuinenburg et al., 2012; Wang-Erlandsson et al., 2018; Wei et al., 2013, 2016)
3. Applications within the context of sustainability and Water Footprinting (Berger et al., 2014, 2018)
4. Understanding the seasonality of precipitation (Guo et al., 2019; Miralles et al., 2016; Zhang et al., 2017) as well as its inter-annual variability (Guo et al., 2019; Keys et al., 2018; Sodemann et al., 2008)
5. Understanding precipitation changes and trends (Zhang et al., 2017, 2019)
6. Investigations into impacts of climate change on the hydrological cycle (Bosilovich et al., 2005; Findell et al., 2019; Singh et al., 2016, 2017)
7. Understanding extreme weather events such as droughts and floods (Dirmeyer and Brubaker, 1999; Drumond et al., 2019; Gangoiti et al., 2011; Gimeno et al., 2016; Herrera-Estrada et al., 2019; Nieto et al., 2019)

The first application refers to moisture supply dependencies for specific regions of interest and comes practically often along with questions related to land cover changes. It can be of importance for regions which mainly rely on rain-fed agriculture where changes in local precipitation could lead very likely to effects on agricultural yields (Van der Ent, 2014; Rockström et al., 2009). Bagley et al. (2012) used in this regard results of a numerical moisture tracking in order to gain knowledge about the sources of precipitation for the major food producing regions in the world. They analyzed the vulnerability of regions towards a decline in crop productivity while including simulations of alterations in land covers of surrounding regions (Bagley et al., 2012). Besides regions of rain-fed agriculture, further regions of interest in research are rainforests or urban areas. Staal et al. (2018) investigated, for instance, cascading moisture recycling effects of the Amazon rainforest whereas Keys et al. (2018) determined the sources of precipitation and water security challenges for various megacities. Next to investigations into moisture supply dependencies and land cover changes, methods and tools within the context of sustainability are listed as a further potential application possibility. One method which could be named in this context is the Water Footprinting which quantifies the water consumption as well as the resulting potential environmental impacts along a product's life cycle (International Organization for Standardization, 2016). First considerations to include moisture tracking in Water Footprinting have been accomplished by Berger et al. (2014, 2018). The last application focus exemplified here refers to a deeper understanding on seasonality aspects as well as the inter-annual variability of precipitation. Guo et al. (2019), for instance, investigated the moisture sources for East Asian precipitation and their temporal variability.

In order to facilitate future applications with regards to atmospheric watersheds, global datasets on the fate of evaporation and the sources of precipitation are needed. However, to our knowledge, only one large-scale approach exists so far which tried to track atmospheric moisture globally over a fine-meshed grid: Dirmeyer et al. (2009) used numerical moisture tracking to determine the sources of precipitation for all land cells across a 1,9° × 1,9° grid. This resulted in an estimation of the source regions of precipitation for most nations as well as major basins in the world made publicly available online (DelSole and Dirmeyer, 2012; Dirmeyer et al., 2009).

A comprehensive and global dataset on the fate of land evaporation was so far not readily available to the broader scientific community. Therefore, the goal of this study is to develop a global scale dataset on the fate of land evaporation for a fine-meshed grid of source and receptor cells which is openly available in a long-term data repository. The results of the study will be presented as source-receptor matrices depicting the yearly average moisture transfers between grid cells. Besides yearly averages, the dataset will comprise monthly averages as well as data in inter-annual resolution. The dataset should enable researchers to gain comprehensive information on the fate of evaporation for any land area of interest covered by the model. Additionally, the goal is to provide information about source-receptor matrices for land areas of a high potential interest such as countries or basins.

2) Material and methods

We used the Eulerian numerical moisture tracking model WAM-2layers (Water Accounting Model-2layers) to create the dataset, which is able to spatially track tagged moisture forward and backward in time - on regional as well as on global scales

(Van der Ent, 2014). The WAM-2layers method as well as its predecessor version has been used extensively (e.g. in Van der Ent and Savenije, 2013; Findell et al., 2019; Guo et al., 2019; Keys et al., 2012, 2018; Keys and Wang-Erlandsson, 2018; Wang-Erlandsson et al., 2018; Zemp et al., 2017; Zhang et al., 2017, 2019; Zhao et al., 2016) and showed results which were consistent with studies using other tracking methods (Van der Ent et al., 2013). We applied the Python version of the model which is available on GitHub (Van der Ent, 2019) and modified pre- and post-processing. The atmospheric moisture tracking was conducted forward in time, thus focusing on the fate of evaporation. The considered grid covered the globe from 79,5° N to 79,5° S latitude. Calculations were performed on a 1,5° latitude × 1,5° longitude grid leading to a total amount of 25680 grid cells (107 × 240). In order to reduce the computational costs, the amount of cells for which the tracking has been applied was reduced to cells which contain land masses or are located within bigger inland lakes (e.g. the Caspian Sea). The land masses of Greenland and Antarctica were excluded, because Eulerian moisture tracking at high latitudes is prone to errors due to high wind speeds compared to the size of the grid cell. As a result, 8684 cells were targeted for the atmospheric moisture tracking. The exact geographical information on the grid and the cells considered for tracking were summarized and are part of the provided dataset.

ERA-Interim (ERA-I) reanalysis data were used as input for the model which are provided by the European Centre for Medium Range Weather Forecasting (ECMWF) (Berrisford et al., 2011; Dee et al., 2011). The considered time horizon for the input data refers to the period of 2000 to 2018. However, the results are going to be presented for the period of 2001 to 2018 as the first year was used as a model spin-up. The following data items were used as input parameters for the model:

- Evaporation, precipitation
- Wind components in zonal and meridional direction
- Specific humidity
- Surface pressure
- Total column water, total column water vapor
- Vertical integral of eastward water vapor flux, vertical integral of eastward cloud liquid water flux, vertical integral of eastward cloud frozen water flux
- Vertical integral of northward water vapor flux, vertical integral of northward cloud liquid water flux, vertical integral of northward cloud frozen water flux

Evaporation and precipitation inputs were incorporated on a three-hourly basis. All other data items were integrated into the model on a six-hourly basis. The download of the data occurred at model levels spanning the atmosphere from zero pressure to surface pressure which are broken down by the model to two layers with well-mixed conditions. Underlying principle of the WAM-2layers model is the water balance shown in Eq. (1) which has been applied in a replicate manner for each time step across the entire grid:

https://doi.org/10.5194/essd-2019-246
Preprint. Discussion started: 27 January 2020

$$\frac{\partial S_k}{\partial t} + \frac{\partial (S_k u)}{\partial x} + \frac{\partial (S_k v)}{\partial y} = E_k - P_k + \xi_k \pm F_v \,, \quad (1)$$

S_k represents the atmospheric moisture storage in layer k and t stands for time. The subscript k stands either for the top or the bottom layer. The variables u and v are describing the wind directions in zonal (x) and meridional (y) directions and represent therefore the horizontal moisture transport between grid cells. Evaporation entering a layer is described by E_k and precipitation removed from a layer by P_k. ξ_k is a residual which is a result of data-assimilation in ERA-I as well as of different spatial and temporal resolution in the calculation steps of the WAM-2layers model. The last term of the equation (F_v) describes the vertical moisture transport between the two layers. Further information on the determination of the single terms of the equation is given in the work of van der Ent et al. (2014).

The main calculations were conducted on the massively parallel computing system of the North-German Supercomputing Alliance (HLRN). During a first post-processing, the results were then aggregated to 13 source-receptor matrices with 8684 × 25680 cells – twelve for the monthly averages and one for the yearly average moisture transfers of the considered time period. Besides the yearly and monthly averages, matrices were also compiled on an inter-annual basis. Table 1 exemplifies the general structure of a source-receptor matrix whereas the diagonal elements represent the moisture which is going to be recycled within the source cell itself.

Table 1 Exemplary source–receptor (evaporation-precipitation) matrix

Source-receptor matrix	Source cell 1	Source cell 2	…	Source cell 8684
Receptor cell 1	…	…	…	…
Receptor cell 2	…	…	…	…
…	…	…	…	…
Receptor cell 25680	…	…	…	…

According to Eq. (2), we verified in each case how well the water balance closes:

$$\Delta_{\text{closure}} = (E_{\text{input}} - E_{\text{assigned}} - L_{\text{north}} - L_{\text{south}} - L_{\text{system}}) \,/\, (E_{\text{input}}) \quad (2)$$

where $\Delta_{closure}$ represents the mismatch within the water balance, E_{input} is the amount of evaporation input, E_{assigned} is water tracked over the considered grid until the point of re-precipitation, L_{north} and L_{south} are unassigned fractions of tracked water which got lost via the system boundaries (latitudes higher than 79,5° N/S) and L_{system} are system losses. The latter term describes unassigned water that is ‘lost’ from the system in the rare case the tracked water would exceed the total water. It may occur especially over mountainous areas or during heavy rainfall whereby the simplified offline tracking does not correspond to the more advanced weather model of ERA-I, or it may be caused by imbalances due to data-assimilation in ERA-I. Mismatches within the water balance could occur because we tracked moisture for all months simultaneously while using the simplified

https://doi.org/10.5194/essd-2019-246
Preprint. Discussion started: 27 January 2020

assumption that the water supply from month N-x to month N will approximately be the same as from month N to month N+x. However, the reality might certainly be characterized in addition by cross-period moisture transfers.

In order to also develop source-receptor matrices for larger regions of interest, moisture transfers of grid cells located within basins or countries were aggregated. Grid cells which contributed only partly to a basin or country were allocated according to the extent of overlap with the respective target area. The described procedure was done with the help of the ArcGis software in which firstly a country and secondly a basin layer was overlain with the 1,5° × 1,5° grid. With regards to countries, the global country boundaries from DIVA-GIS with 265 countries were used which were provided on the ArcGis website (Cun, 2016). We highlight that we do not have any political intentions by referring to this list and that we used it merely as a means of exemplification. Regarding the basins, the basin mask from the Watergap3 model (Eisner, 2016) was applied for the overlaying. Due to geographical boundaries at 79,5° latitude N / S, 8223 basins were considered in total. After the overlaying of the respective maps, the geometric intersections were determined within ArcGis. This was followed by a post-processing in Python dedicated to the creation of the final source-receptor matrices for countries and basins. Finally, the following five types of source-receptor matrices for average moisture transfers were chosen to build the core of the dataset: land grid cell to grid cell, country to grid cell, basin to grid cell, country to country, basin to basin. With regards to the latter two matrices, the quantification of moisture contributions to and from the sea was targeted in addition to moisture transfers between countries respectively basins. This was achieved as follows:

- A country's or basin's share of precipitation originating from the sea was calculated via the difference in total precipitation and the sum of precipitated water originating from countries (or basins)
- A country's or basin's total amount of evaporated water which re-precipitates over the sea was calculated via the difference between the atmospheric moisture recycling over the whole grid and the one taking place over the sum of countries (or the sum of basins).

Finally, usage possibilities of the created dataset were shown via site-specific examples. Examples were chosen with the objective to cover at least all continents and a wide variety of climate zones.

3) Results

3.1) Source-receptor matrices

The gained source-receptor matrices represent the main results of the created dataset. Table 2 specifies the different matrix types, the allocation of source and receptor regions to columns and rows as well as the numbers of matrices.

https://doi.org/10.5194/essd-2019-246
Preprint. Discussion started: 27 January 2020

Table 2 Source-receptor matrices of the created dataset (type 1: land grid cell to grid cell, type 2: country to grid cell, type 3: basin to grid cell, type 4: country to country, type 5: basin to basin)

Type	From (source) – Matrix columns	To (receptor) – Matrix rows	Number of matrices
1	8684 land grid cells	25680 grid cells	13 (monthly + yearly averages) + 18 * 13 (separate inter-annual data for the years 2001 to 2018)
2	265 countries	25680 grid cells	13 (monthly + yearly averages)
3	8223 basins	25680 grid cells	13 (monthly + yearly averages)
4	265 countries + sea	265 countries + sea + unassigned	13 (monthly + yearly averages)
5	8223 basins + sea	8223 basins + sea + unassigned	13 (monthly + yearly averages)

Particularly important is the provision of type 1 matrices within the dataset as they represent the raw data on grid cell basis from which any further aggregation to larger land areas of interest could potentially take place. Together with type 2 (country to grid) and type 3 (basin to grid) matrices, they enable the plotting of evaporationsheds over the whole area of the considered grid. The matrices of type 4 and 5 allow for the generation of self-explanatory source-receptor tables between countries and basins, respectively.

Besides the relevant source-receptor matrices, mismatches within the water balance ($\Delta_{\mathrm{closure}}$) as well as all other terms of Eq. (2) are provided within the dataset. Identified mismatches are in general negligibly small for the annual averages (on average 0.03 % for land grid cells) but reach higher values on a monthly basis (on average 12.6 % for land grid cells). Unassigned fractions of moisture were exclusively allocated to losses via the northern and southern boundaries of the model. Thus, system losses due to storage limits play no role at all.

3.2) Visualization of sample evaporationsheds

Figure 1 to Figure 3 display the yearly average evaporationsheds for three chosen land grid cells, countries and basins. Based on sample scripts provided within the dataset, these types of figures can be plotted for any land grid cell, country or basin of interest. An additional online viewer can be used to directly look up the plots for any land grid cell. Re-precipitation of evaporated water takes place over the whole considered grid and is expressed as a percentage of the evaporated water from the source region. The threshold for the plotting of re-precipitation within different grid cells lies at 0.02 % of the total amount of the assigned water. Additional information with regard to the location, the total evaporation input into the system (E_{input}), the unassigned fractions of water as well as the total share of re-precipitation displayed via the plot are provided seperately via the image captions. Monthly information on moisture transfers for the chosen examples are available within the supporting information (Figure S1 to Figure S36).

https://doi.org/10.5194/essd-2019-246
Preprint. Discussion started: 27 January 2020

Figure 1 shows the evaporationsheds for land grid cells located at Kansas City, US (a), Delhi, India (b) and Kampala, Uganda (c). It exemplifies different possible shapes and geographical extents of evaporationsheds. The evaporationshed for the source cell at Kansas City sprawls, for instance, over large distances and does still not cover more than 70.0 % of the assigned re-precipitation. The evaporationsheds for the source cells at Kampala and Delhi, on the other hand, cover considerably higher shares of the assigned re-precipitation (79.0 % (b), 88.8 % (c)). With regards to the source cell at Kampala, huge amounts of moisture re-precipitate close to the source of evaporation and, thereof, more than 5 % within the source cell itself. Re-precipitation of evaporated water occurs here mainly westwards from the source cell along the equatorial belt and covers huge areas of Central Africa. For the other source cells, moisture recycling takes place mainly eastwards (Kansas City) and southeastwards (Delhi) with lower shares of re-precipitation close to the source of evaporation. The tracking of atmospheric moisture for the source cell at Kansas City led to slight boundary losses due to the loation near to the northern boundary of the model. With regards to Delhi and Kampala, unassigned fractions of moisture due to losses of tagged moisture via the northern or southern boundaries are negligible.

Figure 2 shows evaporationsheds for countries with the examples of Brazil (a), Egypt (b) and Laos (c). Brazil shows a non-fragemented evaporationshed with a huge amount of moisture recycling occuring within the country itself. Egypt's evaporationshed is fragmented with moisture recycling taking place close to the equatorial belt, over the Mediterranean and in the southeast of Europe and Asia. However, hardly any re-precipitation occurs within the country. The evaporationshed of Laos is again non-fragemented with main areas of moisture recycling in Southeast Asia, over the sourrounding sea or in China.

Figure 3 shows example evaporationsheds for basins which refer to parts of the Rio Grande (a), the Danube (b) and the Murray-Darling (c) basin. Core areas of moisture recycling are Central and North America (a), the equatorial belt and huge parts of Eurasia (b), Northern and Eastern Autralia as well as the South Pacific Ocean (c). Displayed evaporationsheds are large while covering only 59.4 to 70.1 % of the assigned moisture recycling.

https://doi.org/10.5194/essd-2019-246
Preprint. Discussion started: 27 January 2020

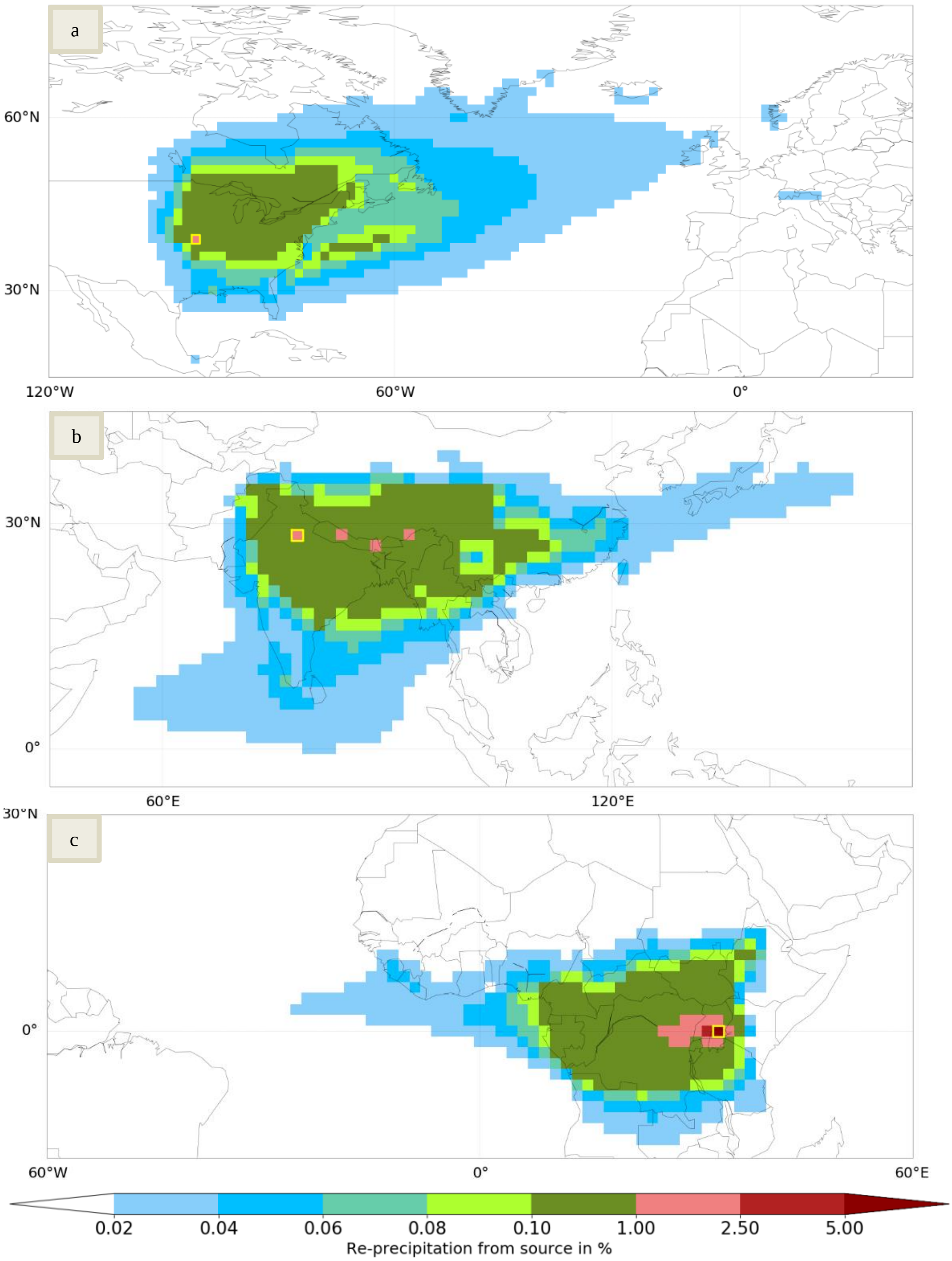

Figure 1 Examples for yearly evaporationsheds of grid cells: a) cell at 39.0° N latitude & 94.5° W longitude (Kansas City, US), E_{input} : 871.6 mm/a, Unassigned : 2.3 %, Colored area covers 70.0 % of the assigned water b) cell at 28.5° N latitude & 78.0° E longitude (Delhi, India), E_{input} : 1132.7 mm/a, Unassigned : 0.1 %, Colored area covers 79.0 % of the assigned water c) cell at 0.0° latitude & 33.0° E longitude (Kampala, Uganda), E_{input} : 1145.1 mm/a, Unassigned : 0.0 %, Colored area covers 88.8 % of the assigned water

https://doi.org/10.5194/essd-2019-246
Preprint. Discussion started: 27 January 2020

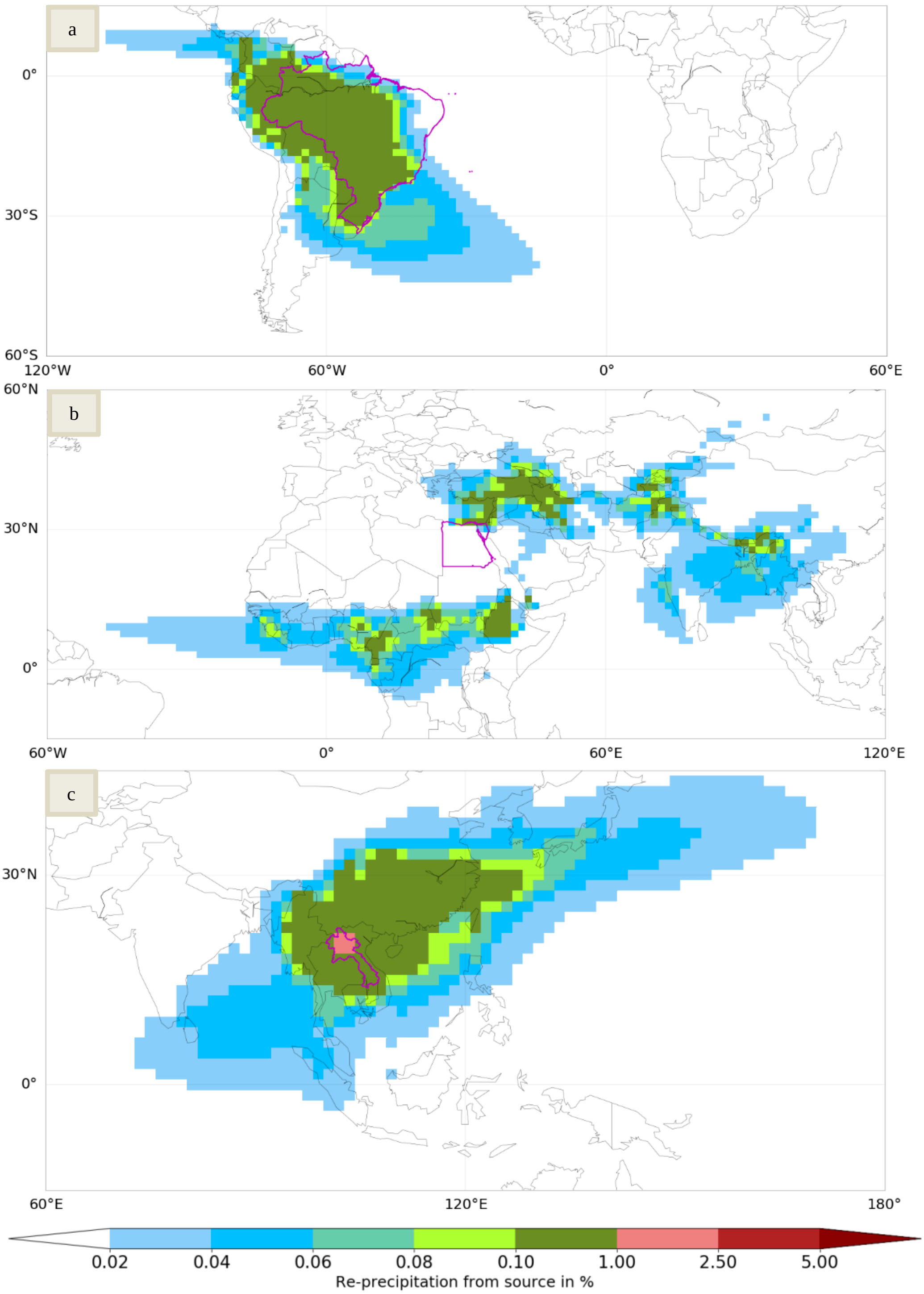

Figure 2 Examples for yearly evaporationsheds of countries a) Brazil – E_{input} : 1240.2 mm/a, Unassigned : 0.1 %, Colored area covers 80.4 % of the assigned water b) Egypt – E_{input} : 104.0 mm/a, Unassigned : 0.8 %, Colored area covers 59.9 % of the assigned water c) Laos – E_{input} : 1178.9 mm/a, Unassigned : 0.4 %, Colored area covers 77.9 % of the assigned water

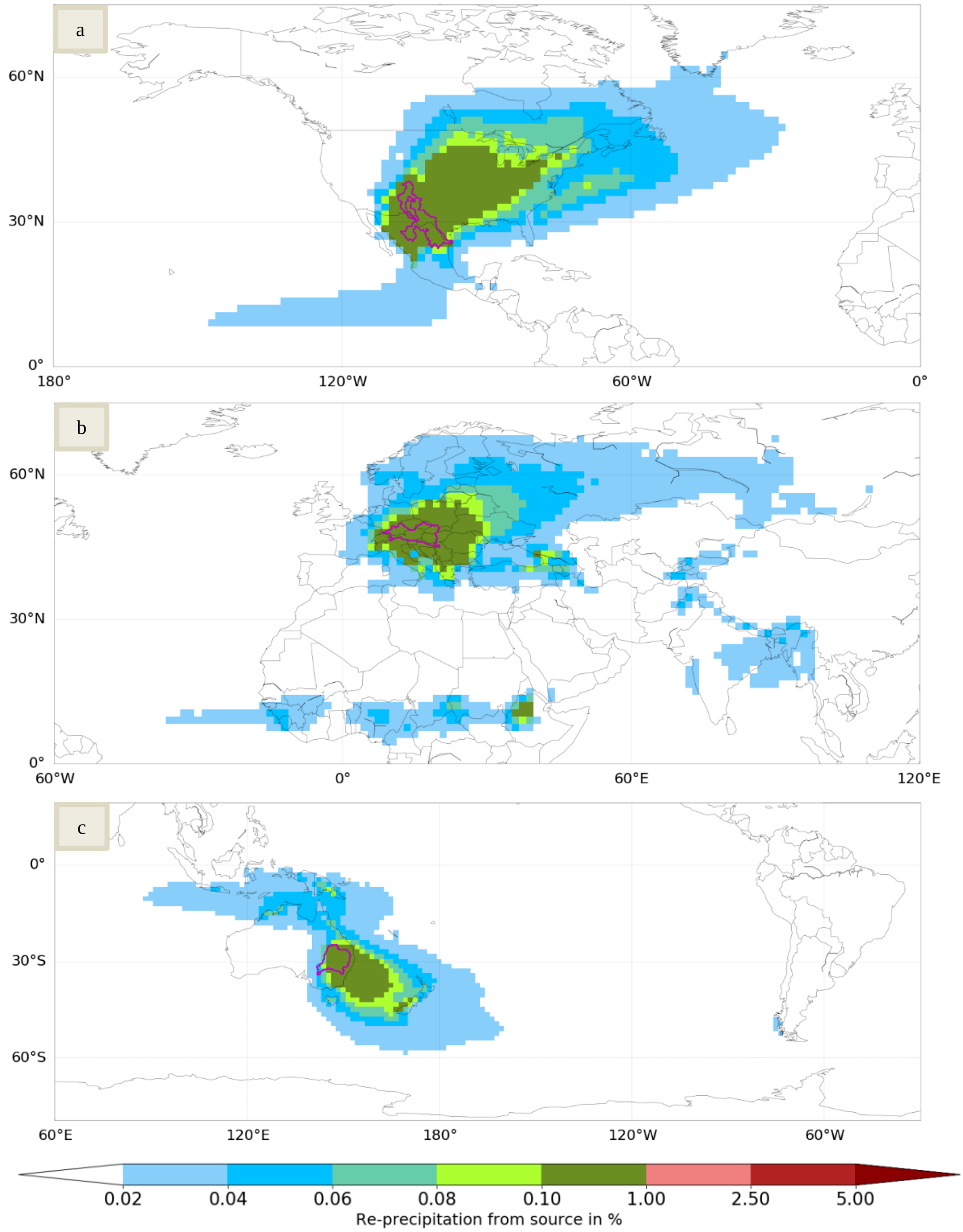

Figure 3 Examples for yearly evaporationsheds of basins a) Basin ID 1463188 (part of the Rio Grande basin) - E_{input} : 502.4 mm/a, Unassigned : 1.3 %, Colored area covers 70.1 % of the assigned water b) Basin ID 1019324 (part of the Danube basin) - E_{input} : 609.4 mm/a, Unassigned : 4.0 %, Colored area covers 60.6 % of the assigned water c) Basin ID 2245569 (part of the Murray-Darling basin) - E_{input} : 503.5 mm/a, Unassigned : 0.5 %, Colored area covers 59.4 % of the assigned water

https://doi.org/10.5194/essd-2019-246
Preprint. Discussion started: 27 January 2020

3.3) Examples for source-receptor tables

Besides the visualization of evaporationsheds, the dataset enables a direct quantification of average moisture transfers between countries or basins within source-receptor tables. This aspect refers to the latter two matrix types (type 4 and 5). At this point type 4 matrices (countries) are used to demonstrate the usage of both types of matrices. Table 3 shows the fate of evaporated water as well as the sources of precipitation for the selected countries. For comparative purposes, the same countries are displayed as for the plotting examples in Figure 2. The presented information is in each case limited to the top 10 sites of re-precipitation and the top 10 sources of precipitation. Values are provided in percent and are related to the total amount of the evaporation or the precipitation input.

Table 3 Fate of evaporation and source of precipitation – Examples for country tables

Brazil Evaporation: 1240.2 mm/a Precipitation: 1868.4 mm/a				**Egypt** Evaporation: 104.0 mm/a Precipitation: 13.1 mm/a				**Laos** Evaporation: 1178.9 mm/a Precipitation: 2176.9 mm/a			
Fate of evaporation		Origin of precipitation		Fate of evaporation		Origin of precipitation		Fate of evaporation		Origin of precipitation	
Site	In %	Site	In %	Site	In %	Site	In %	Site	In %	Site	In %
Brazil	43.6	Sea	63.3	Sea	31.3	Sea	76.6	Sea	44.5	Sea	70.0
Sea	33.6	Brazil	28.9	Russia	7.3	Egypt	2.7	China	26.1	Thailand	6.4
Peru	4.7	Bolivia	1.2	China	5.6	Turkey	1.9	Laos	7.5	Laos	4.1
Colombia	4.5	Peru	0.6	India	5.0	Greece	1.2	Vietnam	5.0	India	3.9
Bolivia	4.3	Argentina	0.6	Ethiopia	4.7	Libya	1.1	Burma	4.2	Burma	3.6
Argentina	4.0	Angola	0.4	Iran	3.5	Sudan / South Sudan	0.9	Thailand	4.2	China	3.4
Paraguay	1.5	Paraguay	0.4	Sudan / South Sudan	3.5	Algeria	0.9	India	1.2	Vietnam	1.9
Ecuador	1.2	Venezuela	0.3	Turkey	3.4	Nigeria	0.8	Russia	1.1	Cambodia	1.3
Venezuela	0.8	Guyana	0.3	Kazakhstan	2.3	United States	0.8	Indonesia	0.9	Indonesia	0.4
Uruguay	0.6	Colombia	0.3	DR Congo	2.2	Italy	0.8	Cambodia	0.8	Russia	0.3

The presented shares with regards to the fate of evaporation are in line with the visualization of evaporationsheds in Figure 2. For Brazil, the highest share of re-precipitation takes place within the country (43.6 %). With regards to Egypt and Laos, the highest share of evaporated water re-precipitates over the sea (Egypt: 31.3 %, Laos: 44.5 %). Concerning additional information on the origin of precipitation, Table 3 highlights the following: In all cases the sea is the biggest source of precipitation with values ranging from 63.3 % (Brazil) to 76.6 % (Egypt). With regards to Brazil and Egypt, the most important terrestrial source of precipitation is the country itself (Brazil: 28.9 %, Egypt: 2.7 %). The most relevant terrestrial evaporative source for the precipitation in Laos is Thailand which supplies on average 6.4 % of the local precipitation.

https://doi.org/10.5194/essd-2019-246
Preprint. Discussion started: 27 January 2020

4) Discussion

4.1) Possible uses of the dataset

The introduction already provided a broad overview on various uses of numerical moisture tracking. In the following it will be summarized for which of the named applications our created dataset could be particularly suitable. The first presented application referred to an increased knowledge on how regions of interest are dependent of the moisture supply from other regions. The provided dataset could provide valuable information to answer those questions, but shows the following limitation: While the dataset includes comprehensive information on the fate of evaporation, information regarding the sources of precipitation are limited to land areas and cannot displayed across the whole grid of land and sea cells. The reason for this is the chosen tracking direction (forward in time) and the focus on land grid cells for the tracking in order to reduce to computational efforts. Nevertheless, the dataset quantifies the amount of precipitation originating from the sea without knowing the exact non-terrestrial source locations. Examples for this were given in Table 3.

The second presented application was related to predictions of potential impacts of human-induced land cover changes on the water cycle. The created dataset could serve as an estimate for the question how land cover changes and altered amounts of land evaporation would potentially affect the supply of water via re-precipitation elsewhere (Keys et al., 2012). Van der Ent et al. (2010) stated within this context that decreasing evaporation (e.g. via deforestation) for areas with high shares of moisture recycling over land "would enhance droughts in downwind areas where overall precipitation amounts are low". The opposing statement to that would also be conceivable – namely that increased land evaporation in these areas could also result in positive water supply effects. Such first-order estimates are relevant in the context of socio-hydrology (Keys and Wang-Erlandsson, 2018; Sivapalan et al., 2012), but we highlight at this point that the dataset can generally not provide more than rough estimates regarding this topic. An exception could be the inspection of inter-annual data for sites where major land cover changes occurred within the covered time period. However, for more comprehensive information on this subject it is advised to apply atmospheric moisture tracking directly to different land cover scenarios.

With regards to the third stated application, sustainability studies and Water Footprinting, the provided dataset shows as well promising usage possibilities. Knowledge on the fate of evaporation was firstly integrated within the method of Water Footprinting by Berger et al. (2014, 2018) via an enhanced water accounting method. This considered atmospheric moisture recycling ratios within drainage basins which could reduce water consumption patterns significantly (Berger et al., 2014, 2018). Aspects of moisture recycling across basin boundaries have not yet been considered so far. The comprehensive information on the fate of land evaporation of the dataset could be used for research regarding this topic.

The fourth possible application was related to research on the variability of precipitation and included seasonal and inter-annual variabilities. As the dataset provides both – monthly data averaged over the considered time period as well as inter-

https://doi.org/10.5194/essd-2019-246
Preprint. Discussion started: 27 January 2020

annual data – it shows a high suitability for this kind of usage. Limitations with regards to the usage of seasonal data could be related to possible mismatches in the water balance which should be verified before usage. However, for the yearly averages those mismatches get negligibly small. The application of studying inter-annual variability is mainly limited to the considered time period (years 2001 to 2018).

Precipitation changes and trends represented the fifth application focus. The dataset can be used in this context to understand changes and trends of moisture recycling for the considered time period whereas predictions into the future are not possible. The sixth and seventh application were related to impacts of climate change on the hydrological cycle and the understanding of extreme weather events. The usage of the dataset for the determination of impacts related to climate change is limited to changes in climate which are reflected by the reanalysis data considered for this study. However, for a deeper analysis of the relationship between global temperature increases and resulting changes in moisture supply patterns, models including scenario analyses would be more suitable. With regards to the understanding of extreme weather events, the dataset could be used in order to gain an increased knowledge on the causes for past droughts. This could be achieved via investigations into anomalies of moisture supply patterns for relevant locations and time periods covered by the model. Investigations into extreme weather events such as floods are on the other side not possible with this dataset as those would require a modeling with a much higher spatial and temporal resolution.

4.2) Comparison to other data sets

At this point a general comparison of our dataset to the existing one referring to the 3D quasi-isentropic back-trajectory (3D QIBT) method (DelSole and Dirmeyer, 2012; Dirmeyer et al., 2009) forced with the NCEP-DOE AMIP-II reanalysis (R-2) (Kanamitsu et al., 2002) and CMAP data (Xie and Arkin, 1997) is given. Next to a slightly higher spatial resolution (1.5° compared to 1.9° resolution), the results of our study are easier to access due to the publication of raw data and aggregated data in a public repository (ready-to-download data). An advantage of the dataset based on the QIBT method is on the other side a longer considered time period (25 years to 18 years). A significant difference is the tracking direction of the two approaches. The QIBT approach traces moisture generally backward in time and its application led to comprehensive information on the sources of precipitation. By contrast, our study focus was on analyzing the fate of evaporation which was realized through a forward tracking of atmospheric moisture. The different tracking directions led to different opportunities for the plotting of atmospheric watersheds. Our dataset enables the plotting of evaporationsheds over the whole considered grid of land and sea cells whereas the plotting of precipitationsheds is limited to the areas of land. Vice versa, the dataset based on the QIBT method enables the plotting of precipitationsheds over the whole considered grid whereas the plotting of evaporationsheds is limited to land cells. In order to exemplify differences of the study outputs, study results on a country level from Dirmeyer et al. (2009) were compared to the results of our dataset based on the following two data items:

https://doi.org/10.5194/essd-2019-246
Preprint. Discussion started: 27 January 2020

- Terrestrial evaporative source (TES = Fraction of precipitation that originated as evaporation from terrestrial sources) according to Dirmeyer et al. (2009)
- Country internal evaporative source (CIES = Fraction of precipitation that originated as evaporation from the same country), which is termed recycling ratio (RR) in Dirmeyer et al. (2009)

Table 4 and Table 5 analyze the top 10 countries with the highest and lowest average TES and CIES values for both datasets. As a general trend our dataset shows in most cases a higher ocean contribution for the evaporative sources of precipitation (derived by in general lower TES values). The main reason for this is probably that the data used by Dirmeyer et al. show a land evaporation which equals on average almost the precipitation over land (ratio of land evaporation to land precipitation: 0.99) and thus allow hardly any runoff (Trenberth et al., 2011; Xie and Arkin, 1997). This fact leads inevitable to TES values (as well as CIES values) which could be classified more on the high side. Moreover, there may be several methodological differences causing different output such as different (vertical) mixing assumptions.

Table 4 Comparison of the top 10 countries with the highest and lowest average TES values between our dataset based on the WAM-2layers method and the one referring to the 3D QIBT method (Dirmeyer et al., 2009) - Countries appearing in both lists are displayed in bold font; CAR = Central African Republic

Rank	Top 10 countries with the highest TES				Top 10 countries with the lowest TES			
	WAM-2layers	in %	3D QIBT	in %	WAM-2layers	in %	3D QIBT	in %
1	**Mongolia**	80.3	**Mongolia**	95.7	**Chile**	4.3	**Chile**	8.1
2	Niger	72.0	**Paraguay**	90.0	**New Zealand**	8.8	**Portugal**	9.9
3	Chad	68.0	Nepal	85.5	**Philippines**	9.3	**New Zealand**	9.9
4	Mali	66.8	Namibia	84.2	**French Guiana**	12.0	Ireland	11.1
5	Cameroon	64.0	Bhutan	84.0	Papua New Guinea	12.2	**Philippines**	11.6
6	Burkina Faso	63.0	Russia	83.2	**Portugal**	12.4	Morocco	12.7
7	Mauritania	62.8	Botswana	82.9	Sri Lanka	13.1	Israel	13.3
8	**CAR**	62.1	Bolivia	82.7	Somalia	14.5	Lebanon	13.7
9	**Paraguay**	61.9	**CAR**	82.0	Suriname	14.8	**French Guiana**	14.5
10	Kyrgyzstan	60.9	Angola	81.3	Belize	15.5	United Kingdom	14.9

https://doi.org/10.5194/essd-2019-246
Preprint. Discussion started: 27 January 2020

Table 5 Comparison of the top 10 countries with the highest and lowest average CIES values between our dataset based on the WAM-2layers method and the one referring to the 3D QIBT method (Dirmeyer et al., 2009) - Countries appearing in both lists are displayed in bold font; CAR = Central African Republic

Rank	Top 10 countries with the highest CIES				Top 10 countries with the lowest CIES			
	WAM-2layers	in %	3D QIBT	in %	WAM-2layers	in %	3D QIBT	in %
1	**Brazil**	28.9	**Russia**	64.7	**Luxembourg**	0.2	**Luxembourg**	0.4
2	**Russia**	27.8	Canada	54.8	**Qatar**	0.3	**Qatar**	0.4
3	**China**	25.9	**Brazil**	46.3	Lebanon	0.5	Belize	0.5
4	**DR Congo**	25.1	**United States**	43.2	**Gambia**	0.8	**Gambia**	0.7
5	Angola	20.9	**China**	41.4	**Israel**	0.8	**Israel**	0.8
6	**Australia**	20.7	**Australia**	37.9	Western Sahara	0.9	Equatorial Guinea	1.2
7	Argentina	19.0	**India**	36.4	Jordan	0.9	**Djibouti**	1.3
8	**United States**	18.3	Mongolia	30.8	**Djibouti**	0.9	El Salvador	1.4
9	**India**	18.1	**DR Congo**	28.5	Belgium	1.0	Macedonia	1.4
10	Sudan / South Sudan	17.4	Mexico	28.4	Iceland	1.0	Rwanda	1.4

Next to general trends, different country compositions can be observed within the lists of the two datasets. Table 4 highlights that only three out of 10 countries appear for both datasets within the list of the 10 highest TES values (Mongolia, the Central African Republic (CAR) and Paraguay). In this context, Mongolia represents in each case the country with the highest share of precipitation originating from terrestrial sources (80.3 % in WAM-2layers, 95.7 % in 3D QIBT). Regarding the countries with the lowest TES values, both approaches list five countries in common (Chile, New Zealand, the Philippines, French Guiana and Portugal) while showing the lowest value for Chile (4.3 % - WAM-2layers, 8.1 % - 3D QIBT). Regarding the CIES (Table 5), high values appear in general for relatively large countries. At this point seven out of 10 countries are listed for both datasets within the top 10 (Brazil, Russia, China, DR Congo, Australia, United States, India). The highest value refers to Brazil (28.9 %) for the WAM-2layers method and to Russia (64.7 %) for the 3D QIBT approach. Small CIES values appear on the other side for relatively small countries. Here we find five countries in common (Luxembourg, Qatar, Gambia, Israel, Djibouti), with Luxembourg showing in each case the lowest value (0.2 % - WAM-2layers, 0.4 % - 3D QIBT). The fact that different countries appear in the tables is most likely caused by spatial differences of evaporation, precipitation and wind speed in the underlying reanalysis input data. A more detailed direct interpretation of differences between individual countries is at this point regarded as out of scope for this paper and could be tackled by comparative studies in the future. The overall comparison of the results with all countries can be gained from the supporting information (Table S1).

5) Data availability

The dataset on the fate of land evaporation is available within the PANGAEA research data repository. It can be accessed through https://doi.pangaea.de/10.1594/PANGAEA.908705 and cited as Link et al. (2019a). The dataset consists of two sub datasets – a basic dataset which contains data averaged over the whole considered time period as well as an inter-annual dataset

https://doi.org/10.5194/essd-2019-246
Preprint. Discussion started: 27 January 2020

providing data for separate years. An attached PDF file ("readme.pdf") explains the structure of the dataset and gives all necessary information on how to work with it. In addition to the provided dataset, a screening tool for the visualization of evaporationsheds on a land grid cell to grid cell basis (based on matrix type 1 of Table 2) can be accessed through http://wf-tools.see.tu-berlin.de/wf-tools/evaporationshed/#/ (Link et al., 2019b).

6) Conclusions

The background of this research was an increased occurrence of studies on the fate and origin of atmospheric moisture. Numerical moisture tracking has been highlighted as one of the main methods to study those aspects. To our knowledge, so far only one approach had been published which tried to track atmospheric moisture globally over a fine-meshed grid (Dirmeyer et al., 2009). This aimed mainly at determining the sources of land precipitation (Dirmeyer et al., 2009). The goal of our study was the provision of a complementary publicly available high resolution global dataset on the fate of land evaporation and was achieved via a global application of the numerical moisture tracking model WAM-2layers. A further post-processing resulted in monthly and yearly source-receptor matrices for average moisture transfers from land grid cells, countries and basins. Furthermore, raw data for inter-annual differences was compiled. The created dataset is the first publicly available dataset ready-to-download providing the overall shape of evaporationsheds for land cells of a global fine-meshed grid in a monthly resolution. Additionally, information on precipitationsheds can be gained via the dataset. The dataset can be regarded as a useful complement to the existing dataset referring to the QIBT method (Dirmeyer et al., 2009; DelSole and Dirmeyer, 2012). It is expected that it will facilitate the access to data on atmospheric moisture recycling and could be integrated into future studies. Possible applications were identified and refer mainly to studies on atmospheric moisture dependencies, impacts of land use changes, Water Footprinting, seasonality and inter-annual variabilities of precipitation, precipitation changes and trends as well as on droughts.

Supplement.

The supplement related to this article is available online at:

Author contributions.

AL, RE: Adaption and testing of the python code, main model run, post-processing - AL, RE, MB: results presentation, plausibility checks, interpretation of the results and compilation of the dataset – AL, RE, MB, MF: Preparation of the manuscript – SE: Provision of the basin mask from the WaterGap3 model as well as advisory support for the post-processing in ArcGis.

https://doi.org/10.5194/essd-2019-246
Preprint. Discussion started: 27 January 2020

Competing interests.

The authors declare that they have no conflict of interest.

Acknowledgements.

The authors acknowledge the HLRN for providing high performance computing resources that have contributed to the research results reported in this paper. Particularly, the support of Dr. Wolfgang Baumann from the HLRN concerning technical and implementation aspects in making the code run on those resources is gratefully acknowledged. Furthermore, the authors acknowledge the support of the German Research Foundation (DFG) who founded this research within the project "Water Footprinting in the Manufacturing Industries – Methods, Tool and Optimization Strategies" (project number: FI 1622/4-1). Ruud van der Ent acknowledges funding from the Netherlands Organization for Scientific Research (NWO), project number 016.Veni.181.015.

References

Bagley, J. E., Desai, A. R., Dirmeyer, P. A. and Foley, J. A.: Effects of land cover change on moisture availability and potential crop yield in the worlds breadbaskets, Environ. Res. Lett., 7(1), doi:10.1088/1748-9326/7/1/014009, 2012.

Berger, M., Van der Ent, R., Eisner, S., Bach, V. and Finkbeiner, M.: Water accounting and vulnerability evaluation (WAVE): Considering atmospheric evaporation recycling and the risk of freshwater depletion in water footprinting, Environ. Sci. Technol., 48(8), 4521–4528, doi:10.1021/es404994t, 2014.

Berger, M., Eisner, S., Van der Ent, R., Flörke, M., Link, A., Poligkeit, J., Bach, V. and Finkbeiner, M.: Enhancing the Water Accounting and Vulnerability Evaluation Model: WAVE+, Environ. Sci. Technol., 52(18), 10757–10766, doi:10.1021/acs.est.7b05164, 2018.

Berrisford, P., Dee, D. P., Poli, P., Brugge, R., Fielding, K., Fuentes, M., Kållberg, P., Kobayashi, S., Uppala, S. and Simmons, A.: The ERA-Interim archive Version 2.0. ERA Report Series 1, [online] Available from: http://www.ecmwf.int/en/elibrary/8174-era-interim-archive-version-20 (Accessed 27 September 2019), 2011.

Bosilovich, M. G., Schubert, S. D. and Walker, G. K.: Global changes of the water cycle intensity, J. Clim., doi:10.1175/JCLI3357.1, 2005.

Cun, J. L.: Global country boundaries, [online] Available from: https://www.arcgis.com/home/item.html?id=2ca75003ef9d477fb22db19832c9554f (Accessed 27 September 2019), 2016.

Dee, D. P., Uppala, S. M., Simmons, A. J., Berrisford, P., Poli, P., Kobayashi, S., Andrae, U., Balmaseda, M. A., Balsamo, G., Bauer, P., Bechtold, P., Beljaars, A. C. M., van de Berg, L., Bidlot, J., Bormann, N., Delsol, C., Dragani, R., Fuentes, M., Geer, A. J., Haimberger, L., Healy, S. B., Hersbach, H., Hólm, E. V., Isaksen, L., Kållberg, P., Köhler, M., Matricardi, M., Mcnally, A. P., Monge-Sanz, B. M., Morcrette, J. J., Park, B. K., Peubey, C., de Rosnay, P., Tavolato, C., Thépaut, J. N. and

https://doi.org/10.5194/essd-2019-246
Preprint. Discussion started: 27 January 2020

Vitart, F.: The ERA-Interim reanalysis: Configuration and performance of the data assimilation system, Q. J. R. Meteorol. Soc., 137(656), 553–597, doi:10.1002/qj.828, 2011.

DelSole, T. M. and Dirmeyer, P. A.: Characterizing Land Surface Memory to Advance Climate Prediction, [online] Available from: http://cola.gmu.edu/wcr/ (Accessed 27 September 2019), 2012.

Dirmeyer, P. A. and Brubaker, K. L.: Contrasting evaporative moisture sources during the drought of 1988 and the flood of 1993, J. Geophys. Res. Atmos., 104(D16), 19383–19397, doi:10.1029/1999JD900222, 1999.

Dirmeyer, P. A., Brubaker, K. L. and DelSole, T.: Import and export of atmospheric water vapor between nations, J. Hydrol., 365(1–2), 11–22, doi:10.1016/j.jhydrol.2008.11.016, 2009.

Dominguez, F., Miguez-Macho, G. and Hu, H.: WRF with water vapor tracers: A study of moisture sources for the North American Monsoon, J. Hydrometeorol., doi:10.1175/JHM-D-15-0221.1, 2016.

Dominguez, F., Hu, H. and Martinez, J. A.: Two-Layer Dynamic Recycling Model (2L-DRM): Learning from Moisture Tracking Models of Different Complexity, J. Hydrometeorol., doi:10.1175/JHM-D-19-0101.1, 2019.

Drumond, A., Stojanovic, M., Nieto, R., Vicente-Serrano, S. M. and Gimeno, L.: Linking Anomalous Moisture Transport And Drought Episodes in the IPCC Reference Regions, Bull. Am. Meteorol. Soc., doi:10.1175/bams-d-18-0111.1, 2019.

Eisner, S.: Comprehensive Evaluation of the WaterGAP3 Model across Climatic, Physiographic, and Anthropogenic Gradients, Ph.D. thesis, University of Kassel, Kassel, 128 pp., 2016.

Findell, K. L., Keys, P. W., van der Ent, R. J., Lintner, B. R., Berg, A. and Krasting, J. P.: Rising Temperatures Increase Importance of Oceanic Evaporation as a Source for Continental Precipitation, J. Clim., doi:10.1175/jcli-d-19-0145.1, 2019.

Gangoiti, G., Gómez-Domenech, I., De Cmara, E. S., Alonso, L., Navazo, M., Iza, J., García, J. A., Ilardia, J. L. and Millán, M. M.: Origin of the water vapor responsible for the European extreme rainfalls of August 2002: 2. A new methodology to evaluate evaporative moisture sources, applied to the August 11-13 central European rainfall episode, J. Geophys. Res. Atmos., doi:10.1029/2010JD015538, 2011.

Gimeno, L., Stohl, A., Trigo, R. M., Dominguez, F., Yoshimura, K., Yu, L., Drumond, A., Durn-Quesada, A. M. and Nieto, R.: Oceanic and terrestrial sources of continental precipitation, Rev. Geophys., 50(4), 1–41, doi:10.1029/2012RG000389, 2012.

Gimeno, L., Dominguez, F., Nieto, R., Trigo, R., Drumond, A., Reason, C. J. C., Taschetto, A. S., Ramos, A. M., Kumar, R. and Marengo, J.: Major Mechanisms of Atmospheric Moisture Transport and Their Role in Extreme Precipitation Events, Annu. Rev. Environ. Resour., 41(1), 117–141, doi:10.1146/annurev-environ-110615-085558, 2016.

Guo, L., Van der Ent, R. J., Klingaman, N. P., Demory, M. E., Vidale, P. L., Turner, A. G., Stephan, C. C. and Chevuturi, A.: Moisture sources for East Asian precipitation: Mean seasonal cycle and interannual variability, J. Hydrometeorol., 20(4), 657–672, doi:10.1175/JHM-D-18-0188.1, 2019.

Herrera-Estrada, J. E., Martinez, J. A., Dominguez, F., Findell, K. L., Wood, E. F. and Sheffield, J.: Reduced Moisture Transport Linked to Drought Propagation Across North America, Geophys. Res. Lett., 46(10), 5243–5253, doi:10.1029/2019GL082475, 2019.

International Organization for Standardization: ISO 14046: Environmental management – Water footprint – Principles, requirements and guidelines (German and English version EN ISO 14046:2016), Geneva., 2016.

Kanamitsu, M., Ebisuzaki, W., Woollen, J., Yang, S. K., Hnilo, J. J., Fiorino, M. and Potter, G. L.: NCEP-DOE AMIP-II reanalysis (R-2), Bull. Am. Meteorol. Soc., doi:10.1175/bams-83-11-1631(2002)083<1631:nar>2.3.co;2, 2002.

Keune, J. and Miralles, D. G.: A precipitation recycling network to assess freshwater vulnerability: Challenging the watershed convention, Water Resour. Res., doi:10.1029/2019wr025310, 2019.

Keys, P. W. and Wang-Erlandsson, L.: On the social dynamics of moisture recycling, Earth Syst. Dyn., 9(2), 829–847, doi:10.5194/esd-9-829-2018, 2018.

Keys, P. W., Van Der Ent, R. J., Gordon, L. J., Hoff, H., Nikoli, R. and Savenije, H. H. G.: Analyzing precipitationsheds to understand the vulnerability of rainfall dependent regions, Biogeosciences, 9(2), 733–746, doi:10.5194/bg-9-733-2012, 2012.

Keys, P. W., Wang-Erlandsson, L. and Gordon, L. J.: Megacity precipitationsheds reveal tele-connected water security challenges, PLoS One, 13(3), 1–22, doi:10.1371/journal.pone.0194311, 2018.

Link, A., Van der Ent, R., Berger, M., Eisner, S. and Finkbeiner, M.: The fate of land evaporation - A global dataset, PANGAEA, https://doi.pangaea.de/10.1594/PANGAEA.908705, 2019a.

Link, A., Van der Ent, R., Berger, M., Eisner, S. and Finkbeiner, M.: Tool for Visualizing the Fate of Land Evaporation, [online] Available from: https://wf-tools.see.tu-berlin.de/wf-tools/evaporationshed/#/ (Accessed 16 December 2019), 2019b.

Miralles, D. G., Nieto, R., McDowell, N. G., Dorigo, W. A., Verhoest, N. E. C., Liu, Y. Y., Teuling, A. J., Dolman, A. J., Good, S. P. and Gimeno, L.: Contribution of water-limited ecoregions to their own supply of rainfall, Environ. Res. Lett., 11(12), 1–12, doi:10.1088/1748-9326/11/12/124007, 2016.

Nieto, R., Ciric, D., Vázquez, M., Liberato, M. L. R. and Gimeno, L.: Contribution of the main moisture sources to precipitation during extreme peak precipitation months, Adv. Water Resour., doi:10.1016/j.advwatres.2019.103385, 2019.

Rockström, J., Falkenmark, M., Karlberg, L., Hoff, H., Rost, S. and Gerten, D.: Future water availability for global food production: The potential of green water for increasing resilience to global change, Water Resour. Res., 45(7), 1–16, doi:10.1029/2007WR006767, 2009.

Salih, A. A. M., Zhang, Q., Pausata, F. S. R. and Tjernström, M.: Sources of Sahelian-Sudan moisture: Insights from a moisture-tracing atmospheric model, J. Geophys. Res., doi:10.1002/2015JD024575, 2016.

Singh, H. K. A., Bitz, C. M., Donohoe, A., Nusbaumer, J. and Noone, D. C.: A mathematical framework for analysis of water tracers. Part II: Understanding large-scale perturbations in the hydrological cycle due to CO 2 doubling, J. Clim., doi:10.1175/JCLI-D-16-0293.1, 2016.

Singh, H. K. A., Bitz, C. M., Donohoe, A. and Rasch, P. J.: A source-receptor perspective on the polar hydrologic cycle: Sources, seasonality, and arctic-antarctic parity in the hydrologic cycle response to CO 2 doubling, J. Clim., doi:10.1175/JCLI-D-16-0917.1, 2017.

Sivapalan, M., Savenije, H. H. G. and Blöschl, G.: Socio-hydrology: A new science of people and water, Hydrol. Process., doi:10.1002/hyp.8426, 2012.

Sodemann, H., Schwierz, C. and Wernli, H.: Interannual variability of Greenland winter precipitation sources: Lagrangian moisture diagnostic and North Atlantic Oscillation influence, J. Geophys. Res. Atmos., doi:10.1029/2007JD008503, 2008.

Spracklen, D. V., Arnold, S. R. and Taylor, C. M.: Observations of increased tropical rainfall preceded by air passage over forests, Nature, 489(7415), 282–285, doi:10.1038/nature11390, 2012.

Staal, A., Tuinenburg, O. A., Bosmans, J. H. C., Holmgren, M., Van Nes, E. H., Scheffer, M., Zemp, D. C. and Dekker, S. C.: Forest-rainfall cascades buffer against drought across the Amazon, Nat. Clim. Chang., doi:10.1038/s41558-018-0177-y, 2018.

Trenberth, K. E., Fasullo, J. T. and Mackaro, J.: Atmospheric moisture transports from ocean to land and global energy flows in reanalyses, J. Clim., doi:10.1175/2011JCLI4171.1, 2011.

Tuinenburg, O. A., Hutjes, R. W. A. and Kabat, P.: The fate of evaporated water from the Ganges basin, J. Geophys. Res. Atmos., doi:10.1029/2011JD016221, 2012.

Van der Ent, R. J.: A new view on the hydrological cycle over continents, Ph.D. thesis, Delft University of Technology, Delft, 96 pp., 2014.

Van der Ent, R. J.: WAM-2layers python, [online] Available from: https://github.com/ruudvdent/WAM2layersPython (Accessed 27 September 2019), 2019.

Van der Ent, R. J. and Savenije, H. H. G.: Oceanic sources of continental precipitation and the correlation with sea surface temperature, Water Resour. Res., 49(7), 3993–4004, doi:10.1002/wrcr.20296, 2013.

Van der Ent, R. J., Savenije, H. H. G., Schaefli, B. and Steele-Dunne, S. C.: Origin and fate of atmospheric moisture over continents, Water Resour. Res., 46(9), 1–12, doi:10.1029/2010WR009127, 2010.

Van der Ent, R. J., Tuinenburg, O. A., Knoche, H. R., Kunstmann, H. and Savenije, H. H. G.: Should we use a simple or complex model for moisture recycling and atmospheric moisture tracking?, Hydrol. Earth Syst. Sci., 17(12), 4869–4884, doi:10.5194/hess-17-4869-2013, 2013.

Van Der Ent, R. J., Wang-Erlandsson, L., Keys, P. W. and Savenije, H. H. G.: Contrasting roles of interception and transpiration in the hydrological cycle – Part 2: Moisture recycling, Earth Syst. Dyn., doi:10.5194/esd-5-471-2014, 2014.

Wang-Erlandsson, L., Fetzer, I., Keys, P. W., Van Der Ent, R. J., Savenije, H. H. G. and Gordon, L. J.: Remote land use impacts on river flows through atmospheric teleconnections, Hydrol. Earth Syst. Sci., 22(8), 4311–4328, doi:10.5194/hess-22-4311-2018, 2018.

Wei, J., Dirmeyer, P. A., Wisser, D., Bosilovich, M. G. and Mocko, D. M.: Where does the irrigation water go? An estimate of the contribution of irrigation to precipitation using MERRA, J. Hydrometeorol., doi:10.1175/JHM-D-12-079.1, 2013.

Wei, J., Knoche, H. R. and Kunstmann, H.: Atmospheric residence times from transpiration and evaporation to precipitation: An age-weighted regional evaporation tagging approach, J. Geophys. Res., doi:10.1002/2015JD024650, 2016.

Xie, P. and Arkin, P. A.: Global Precipitation: A 17-Year Monthly Analysis Based on Gauge Observations, Satellite Estimates, and Numerical Model Outputs, Bull. Am. Meteorol. Soc., doi:10.1175/1520-0477(1997)078<2539:GPAYMA>2.0.CO;2, 1997.

Zemp, D. C., Schleussner, C. F., Barbosa, H. M. J., Hirota, M., Montade, V., Sampaio, G., Staal, A., Wang-Erlandsson, L. and Rammig, A.: Self-amplified Amazon forest loss due to vegetation-atmosphere feedbacks, Nat. Commun., 8, 1–10, doi:10.1038/ncomms14681, 2017.

Zhang, C., Tang, Q. and Chen, D.: Recent changes in the moisture source of precipitation over the tibetan plateau, J. Clim., doi:10.1175/JCLI-D-16-0493.1, 2017.

Zhang, C., Tang, Q., Chen, D., Van der Ent, R. J., Liu, X., Li, W. and Haile, G. G.: Moisture source changes contributed to different precipitation changes over the northern and southern Tibetan Plateau, J. Hydrometeorol., doi:10.1175/JHM-D-18-0094.1, 2019.

Zhao, L., Liu, X., Wang, N., Kong, Y., Song, Y., He, Z., Liu, Q. and Wang, L.: Contribution of recycled moisture to local precipitation in the inland Heihe River Basin, Agric. For. Meteorol., 271(March), 316–335, doi:10.1016/j.agrformet.2019.03.014, 2019.

Zhao, T., Zhao, J., Hu, H. and Ni, G.: Source of atmospheric moisture and precipitation over China's major river basins, Front. Earth Sci., 10(1), 159–170, doi:10.1007/s11707-015-0497-4, 2016.